RESEARCH

Characterization of recombinant humanized collagen type III and its influence on cell behavior and phenotype

Jing Wang[1,2], Hong Hu[1,2], Jian Wang[3], He Qiu[4], Yongli Gao[1,2], Yang Xu[1,2], Zhanhong Liu[1,2], Yajun Tang[1,2], Lu Song[1,2], John Ramshaw[5], Hai Lin[1,2*] and Xingdong Zhang[1,2]

Abstract

Collagen made a tremendous impact in the field of regenerative medicine as a bioactive material. For decades, collagen has been used not only as a scaffolding material but also as an active component in regulating cells' biological behavior and phenotype. However, animal-derived collagen as a major source suffered from problems of immunogenicity, risk of viral infection, and the unclear relationship between bioactive sequence and function. Recombinant humanized collagen (rhCol) provided alternatives for regenerative medicine with more controllable risks. However, the characterization of rhCol and the interaction between rhCol and cells still need further investigation, including cell behavior and phenotype. The current study preliminarily demonstrated that recombinant humanized collagen type III (rhCol III) conformed to the theoretical amino acid sequence and had an advanced structure resembling bovine collagen. Furthermore, rhCol III could facilitate basal biological behaviors of human skin fibroblasts, such as adhesion, proliferation and migration. rhCol III was beneficial for some extracellular matrix-expressing cell phenotypes. The study would shed light on the mechanism research of rhCol and cell interactions and further understanding of effectiveness in tissue regeneration.

Keywords: Recombinant collagen, Collagen type III, Advanced structure, Cell behavior, Cell phenotype

*Correspondence: ohai3@163.com

[1] National Engineering Research Center for Biomaterials, Sichuan University, Chengdu 610064, Sichuan, China
Full list of author information is available at the end of the article

Wang *et al. Journal of Leather Science and Engineering*   (2022) 4:33

Page 2 of 13

Graphical abstract
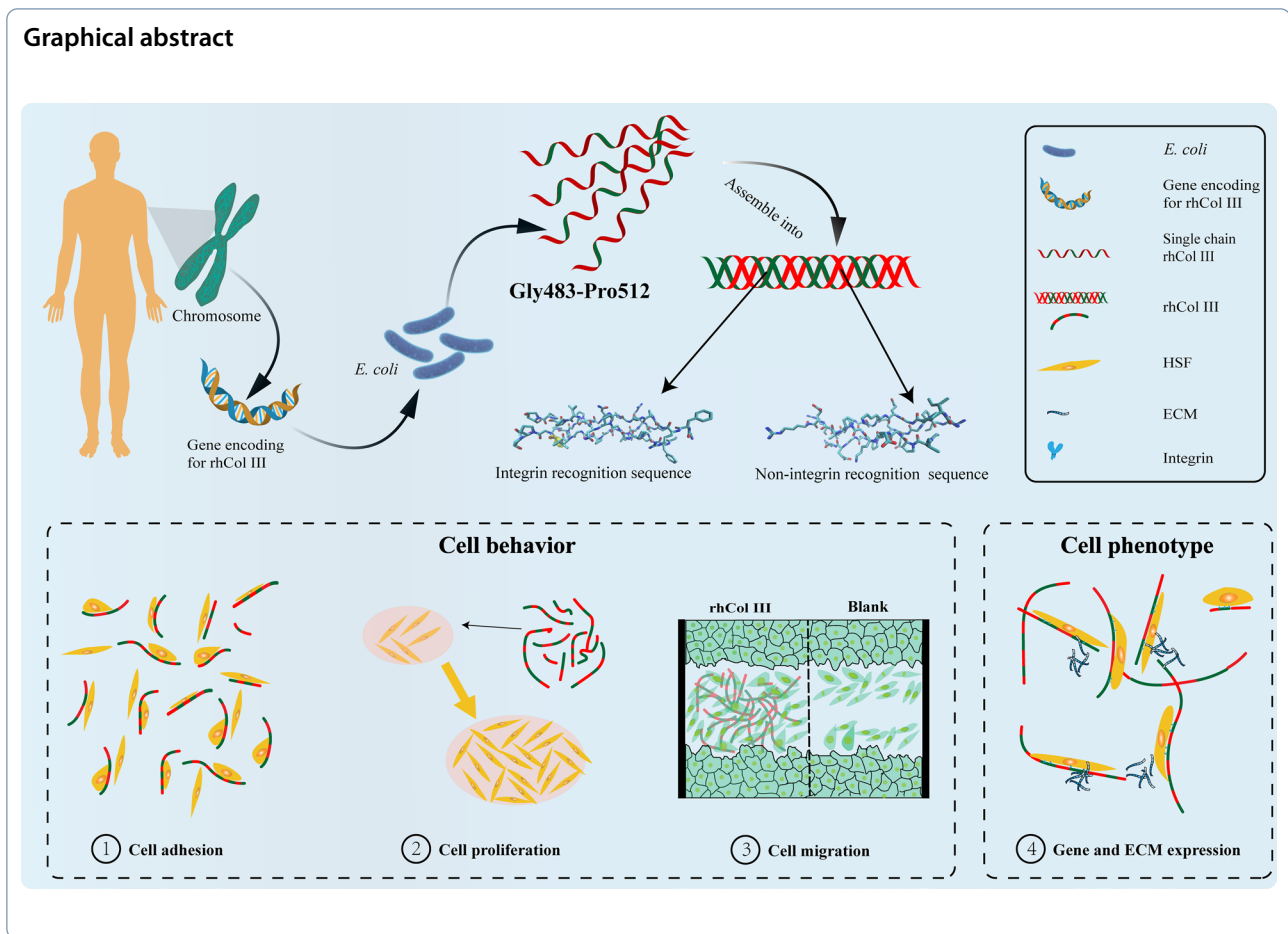
1 Introduction

The interaction between cells and collagen is essential in the process of tissue development, disease, aging and even death [1–4]. Comprehension of the collagen and cell interactions is beneficial to searching for alternative strategies to achieve delayed aging, disease treatment, and tissue repair. However, native collagen is a big and complex protein family; even a single collagen molecule is composed of thousands of amino acids and abundant advanced structures. Given subtype and quaternary structures, animal-derived collagen contains multiple bioactive regions so it is challenging to identify the relationship between individual bioactive region and cell [5]. Furthermore, animal-derived collagen is subjected to the risk of immunogenicity and viral infection when it is applied as heterologous starting material for implants or medical devices [6]. The limitations of native collagen set obstacles to the wide application of collagen-based biomaterials.

Genetic recombination technologies have been utilized to express different types of recombinant collagen or collagen-like proteins in bacterial or fungal hosts over the past 2 decades [7, 8]. With the assistance of modern computational simulations, more bioactive amino acid sequences or collagen segments could be identified and screened for further studies. Thus, recombinant collagen with screened or designed amino acid sequences could have specific bioactivity with high purity and low batch variation. At the same time, recombinant collagen has some shortcomings such as inadequate stability, fast degradation rate, insufficient mechanical properties, etc. [9]. The reasons are various, and one of the strategies to compensate the weakness is introducing additional amino acid sequences to form a triple helix or higher-order collagen-like structures [10–13]. In other words, amino acid segments for increasing bioactivity and structural stability may co-exist in the recombinant collagen to improve the application performance.

To date, more than ten different recombinant collagens have been shown to have a triple helix structure [14–16]. The retention of the recombinant collagen triple helix structure is crucial in ensuring that the material has a chemotactic function and high biological activity inherited from animal collagen [10, 16, 17]. For recombinant

Wang *et al. Journal of Leather Science and Engineering*   (2022) 4:33

Page 3 of 13

collagen, the hydroxyproline acid (Hyp) content largely determines the triple helix's stability. However, Hyp is not a sufficient condition for forming the triple helix structure. Xu's [18] team reported that *E. coli* lacking proline hydroxylase could express recombinant collagen with a triple helix structure. In tissues, triple-helix structures could be further assembled into more advanced supramolecular structures, known as the D-period. The D-period is an essential feature of collagen and is related to the biomechanical properties of the extracellular matrix (ECM) [19]. The investigators found that recombinant collagen also has the potential to assemble into collagen fibers with D-period and noted that the periodicity of the sequence facilitates further assembly of the D-period [16]. Overall, recombinant collagen may form a multilevel structure similar to animal collagen by proper design.

Traditionally, collagen was considered to be a bio-inert ECM, functioning as a space-filling material to provide mechanical support and tissue integrity [20]. However, in recent years, it has been found that collagen contained a wide repertoire of bioactive sites, which interacted with receptors on the cell membrane surface to regulate the biological behavior of the cells [21]. These bioactive sites included all GxxGEx [22] integrin recognition sequences presented in collagen, such as GFOGER, GAOGER, GLOGER, and so on [23]. In addition, the collagen also comprised binding sites for discoidin domain receptors [24], OSCAR [25], A3 domain of vWF [26], LAIR-1 [27], Glycoprotein VI [28]. These receptors were involved in cell adhesion, proliferation, migration, inflammation activation, immune regulation, platelet activation, and tissue remodeling [23]. Therefore, recombinant collagen could be designed with the required functional and structural sequences depending on the actual context [29]. This "bottom–up" design of collagen structure and biological function opened the gateway to the application of collagen-based materials in the field of regenerative medicine.

In our previous study, rhCol III could modulate cell biological behavior and promote ECM expression to alleviate skin injury from photoaging in vivo [30]. In addition, rhCol III was used as a bioactive material in combination with a scaffold or carrier for chronic wound treatment [31]. There is still a knowledge gap in the study of rhCol III, in terms of validating its multi-level structure and its effect on the basic biological behavior and ECM expression of fibroblasts. In this study, the characterization of rhCol III was mainly focused on the component and structure, including the molecular weight, amino acid contents and their consistency with the theoretical design. Subsequently, the influence of rhCol III on human skin fibroblast (HSF) behavior was investigated, containing cell adhesion, proliferation, and migration. Finally, the promotive effects of rhCol III on the secretion of various extracellular matrices were explored by RT-qPCR and ELISA at the gene and protein levels. This study would provide detailed evidence to fill in the knowledge gap of understanding how designed rhCol could influence cell behavior, which might provide a strategy for tissue regeneration. This study would provide detailed evidence to fill in the knowledge gap of understanding how designed rhCol could influence cell behavior, which might provide a strategy for tissue regeneration.

2 Materials and methods
2.1 Materials
The lyophilized recombinant humanized collagen type III (rhCol III) was provided by Shanxi Jinbo Pharmaceutical Co., Ltd. The structural information of rhCol III is indexed by the Global Protein Data Bank with PDB ID 6A0A and 6A0C. Human skin fibroblast cell (HSF) was purchased from the National Collection of Authenticated Cell Cultures, Shanghai, China. Isopropyl alcohol was purchased from Chron Chemicals, China. Phosphate buffered saline (PBS) powder was provided by Servicebio, Wuhan, China. The preparation of bovine type I collagen was referred to an issued patent (China Patent No. CN109731136B). The characterization of bCol I was referred to Chinese pharmaceutical industry standard YY 0954-2015 and bCol I met the requirements was applied in this study.

2.2 Characterization of rhCol III
2.2.1 Amino acid contents
The determination of amino acid content was referred to the assay method in GB 5009.124-2016 (a National Standard of the People's Republic of China) with slight modifications. Briefly, 2 mL of rhCol (0.872 mg/mL) was hydrolyzed in 8 mL 6 M HCl in an ampoule at 115 °C for 22 h; the test sample was prepared by vacuum drying the hydrolysate and dissolving to constant volume with double distilled water in a volumetric flask. A Hitachi LA8080 automatic amino acid analyzer (Tokyo, Japan) was utilized to determine the amino acid contents in rhCol III.

2.2.2 Molecule weight and distribution
2.2.2.1 Mass spectrometry (HPLC–MS) The molecule weight and its distribution of rhCol III were determined by high performance liquid chromatography–mass spectrometry (HPLC–MS). Briefly, rhCol III was dissolved with water to a concentration of 1 mg/mL. The attained rhCol III solution was separated on BioResolve RP mAb Columns (450A, 2.7 μm particle size, 3 mm × 100 mm). The mobile phase A was 0.1% TFA in double distilled water, and B was 0.1% TFA in acetonitrile. The sample

was loaded by the autosampler with 2 μL and separated by the column with a flow rate of 0.3 mL/min and UV detection at 210 nm. Samples were analyzed with a XevoG2-XS QTof mass spectrometer. Detection mode: positive ion scan, precursor scan, range: 500–4000 m/z. The raw data were processed by UNIFI (1.8.2, Waters) software with the following parameter settings (Table 1).

2.2.3 Structure identification

The rhCol III samples were dissolved in PBS buffer (10 mM, pH 7.4) at a concentration of 1 mg/mL and held overnight at 4 ℃ before analyzing by circular dichroism spectroscopy, which was equipped with a Jasco J-1500 spectropolarimeter [32]. The spectra were collected with three accumulations at the wavelength of 190 nm to 300 nm, the path length of 0.1 cm, and a scanning speed of 50 nm/min. The baseline correction was performed using a PBS buffer.

The freeze-dried bovine collagen type I (bCol I, laboratory self-made) and rhCol III sponges were used for Fourier transform infrared assay using Nicolet iS50 (Thermo Fisher, USA). The background and samples were scanned 64 times in the wavenumber range of 4000 cm^{-1}–400 cm^{-1} with a resolution of 4 cm^{-1}. The spectra were processed by automatic baseline calibration and 9 points smoothing for further analysis.

2.3 Influence on cell behavior

2.3.1 Cell adhesion

The cell specifically adhered to the two-dimensional surface was quantified to evaluate the cell adhesion activity of the material, as described previously [33]. HSF was used in the assay, and the sample solutions were prepared by dissolving the rhCol III, bCol I at a concentration of 0.5 mg/mL, respectively. PBS buffer was used as blank control. The sample solutions were added to 96-well microplates (CLS9018, corning, USA) at 100 μL/well, and sufficient protein would be deposited on the well surface after being placed at 4 ℃ overnight. Then, the well was washed 2–3 times with PBS to remove non-adsorbed proteins, following an addition of 100 μL heat-inactivated BSA and incubation at 37 ℃ for 1 h to avoid non-specific cell adhesion. After rinsing the wells with PBS buffer, HSF was seeded at the density of

1×10^5 cells/mL and cultured for 1 h. Subsequently, the non-adhered cells were washed off with PBS and incubated with 100 μL of DMEM medium containing 10% Cell Counting Kit-8 (Biosharp, Labgic Technology Co., Ltd., China) for 30 min. The absorbance at 450 nm was read and recorded using a microplate spectrophotometer (ThermoMax Microplate Reader, Molecular Devices).

2.3.2 Cell proliferation

The influence of rhCol III on HSF proliferation was studied using a Cell Counting Kit-8 method. Briefly, the HSF were seeded at 5,000 cells per well in a 96-well plate and cultured overnight in DMEM complete medium. Then, the medium was replaced by the medium containing rhCol III with a concentration of 0.01 mg/mL, 0.10 mg/mL and 1.00 mg/mL, respectively. After culturing for 1, 3, 5, and 7 days, CCK-8 kit was applied, and the solution absorbance was measured at 450 nm to evaluate the cell proliferation, while a parallel group without rhCol III was severed as the blank control.

2.3.3 Cell migration

The cell migration assay using HSF was conducted following standard protocol. Firstly, 5000 cells/well HSF were seeded in a separate culture chamber of the Culture-Insert (Ibidi, Gräfelfing, Germany) and cultured to 95% confluency. After removing the silicone barrier from the center of the Culture-Insert, the wells were washed with PBS buffer to eliminate the dead cells. Serum-free DMEM with or without rhCol III (0.2 mg/mL) was added to the well. The cell migration was imaged at different time points by a digital camera installed on an inverted microscope. According to the results assessed by Image-Pro Plus Version 6.0 software, cell migration was quantitatively evaluated by relative migration rate using the following formula:

$$\text{Relative migration rate (\%)} = \frac{A_0 - A_t}{A_0} * 100\%$$

where A_0 represented the initial scratch width, and A_t meant the scratch width after culturing for t hours, that was 24 or 72 h in this study, respectively.

2.4 Influence on cell phenotype

2.4.1 Gene expression determined by real-time quantitative PCR (RT-qPCR)

RT-qPCR was used to quantitatively analyze the expression of type I, III, IV and VII collagen expressed by fibroblasts. Total RNA was extracted using the RNAprep pure Cell/Bacteria Kit (Tiangen Biotech, Beijing, China) according to the manufacturer's protocol. cDNA template for PCR amplification was prepared by reverse transcription of total RNA (1000 ng) using the

Table 1 MaxEnt1 processing

Peak width model	TOF
TOF resolution	10,000
Input m/z range	700–1200
Output resolution	0.25 Da
Iterations	15

Table 2 Primers for RT-qPCR Analysis

	Forward	Reverse
Collagen I	F:5′-GTGGCAGTGATGGAAGTGTG-3′	R:5′-AGGACCAGCGTTACCAACAG-3′
Collagen III	F:5′-ACCAGGAGCTAACGGTCTCA-3′	R:5′-TCTGATCCAGGGTTTCCATC-3′
Collagen IV	F:5′-AGGTGTCATTGGGTTTCCTG-3′	R:5′-GGTCCTCTTGTCCCTTTTGTT-3′
Collagen VII	F:5′-ACTGTGATTGCCCTCTACGC-3′	R:5′-GGCTGTGGTATTCTGGATGG-3′
GAPDH	F:5′-AGACAGCCGCATCTTCTTGT-3′	R:5′-TTCCCATTCTCAGCCTTGAC-3′

RevertAid RT Reverse Transcription kit (Thermo Scientific, USA). The specific primers used for RT-qPCR analysis (Table 2) were synthesized by Qingke Biology (Chengdu, China). As recommended by the official instruction manual, following thermal cycling was used. RT-qPCR was performed using the CFX96TM real-time PCR detection system (Bio-Rad, USA) with $2 \times$ EasyTaq® PCR SuperMix Supermix (TransGen Biotech, Beijing, China). The gene expression level of each targeted gene was determined by the $2^{-\Delta\Delta CT}$ method. Target gene mRNA expression levels were normalized to the housekeeping gene GAPDH as an internal control for quantification.

2.4.2 Extracellular matrix expression evaluated by enzyme linked immunosorbent assay (ELISA)

Fibroblast cells were cultured in DMEM medium with 15% fetal bovine serum (Hyclone, UT, USA), 1% penicillin−streptomycin (Hyclone, USA) and 0.2 mg/mL of rhCol III under a 5% CO_2 humidified atmosphere at 37 °C, for 1 and 3 days. The cultured supernatant was collected to measure the contents of hyaluronic acid (HA) and type I collagen, respectively. The concentration of type I collagen and hyaluronic acid was measured by ELISA (Zhuocai Biotechnology Ltd., Shanghai, China). The absorbance at 450 nm was measured using a microplate spectrophotometer.

2.5 Statistical analysis

All data are presented as mean ± standard deviation (n ≥ 3). Statistical analysis was performed using one-way ANOVA unless otherwise noted. The differences between groups of $*p < 0.05$, $**p < 0.01$, $***p < 0.001$ and $****p < 0.0001$ were considered significant.

3 Results

3.1 Characterization of rhCol III

rhCol III applied in this study was encoded by a gene segment of human collagen type III (COL3A1_Human (Uniprot ID: P02461) Gly483-Pro512, Single repeat amino acid sequence GERGAP GFRGPA GPNGIP GEKGPA GERGAP) and further expressed by *E.coli* with 16 times repeat [34]. The theoretical molecular weight of rhCol III was 44,755, Da according to the amino acid components in the sequence.

The mass spectrometry results presented in Fig. 1 suggested a high purity of rhCol III and very narrow distribution of molecule weight. According to the mass spectrum, the molecular weight of rhCol III was
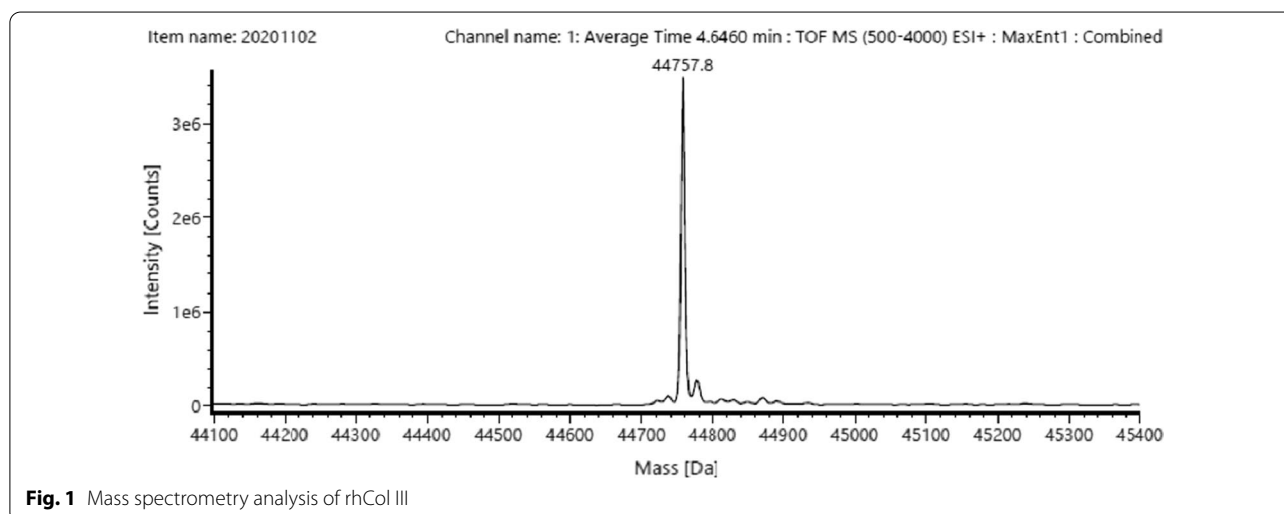

Fig. 1 Mass spectrometry analysis of rhCol III

Wang *et al. Journal of Leather Science and Engineering*   (2022) 4:33

Page 6 of 13

primary at 44,757.8 Da, which validated the agreement with the theoretical molecular weight 44,754.93 Da. The slight deviation of molecular weight from theoretical value might because of the different protonation degree of the side groups, which included guanidine group (pKa = 12.10) and amino group (pKa = 4.15) according to the amino acid sequence in the repeat unit of rhCol III.

The amino acid contents of rhCol III were shown in Table 3. Nine amino acids were detected in rhCol III, and the contents were very close to the theoretical values, which could be calculated according to the amino acid sequence of segment Gly483-Pro512 in human collagen type III. Meanwhile, no additional amino acid such as histidine (His) was detected in rhCol III, which meant no protein tag was included in the recombinant collagen since His was only utilized in the protein tags.

Circular dichroism was used to assess the presence of the triple helix structure in rhCol III and the stability of the triple helix structure compared to bCol I. As shown in Fig. 2, the circular dichroism spectra revealed that both the rhCol III and bCol I possessed advanced structure characteristics, as evidenced by the negative peak near 207–208 nm and the positive peak near 221–222 nm [35]. Therefore, it could be inferred that rhCol III might have similar advanced structures as native bCol I, which had the triple helix as a principle feature. In addition, the ratio of the positive peak intensity to that of the negative peak (Rpn) was usually used to evaluate the triple helix content in advanced structures of collagen [10]. In this study, Rpn values of rhCol III and bCol I were 0.24 and 0.48, respectively.

FTIR spectroscopy (Fig. 3) was used to verify the rhCol III triple helix structure and the structural differences between rhCol III and bCol I. The characteristic peaks of collagen, such as amide A, amide B, amide I, amide II and amide III are considered to be associated with
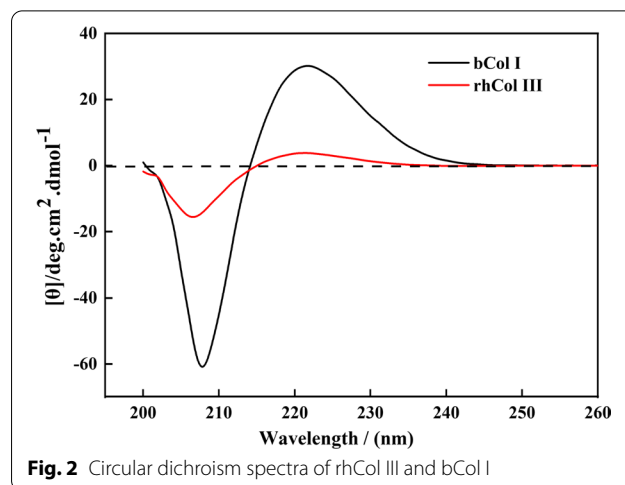
Fig. 2 Circular dichroism spectra of rhCol III and bCol I
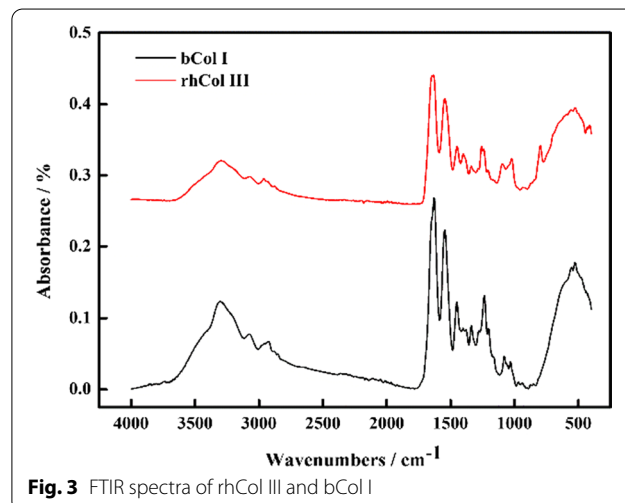
their secondary structures. As could be seen in Table 4, rhCol III and bCol I showed the same wavenumber of the amide I band, and the amide III in rhCol III blue-shifted and had an individual absorption peak at 1260 cm^{-1}, which might attribute to the random coil components as reported [36]. The Amide III / A1450 of rhCol III was lower than that of bCol I demonstrating the low content of triple helix structures in rhCol III compared to bCol I, which was consistent with the CD spectroscopy results. Furthermore, the amide A band of rhCol III was red-shifted, which suggested that rhCol III involved more hydrogen bonds in maintaining the triple helix structure compared to bCol I [37].

3.2 Influence of rhCol III on cell behaviors

The recognition of contact sites on collagen and interactions between cell and extracellular matrix were imperative for cell behaviors and phenotype, including

Table 3 Amino acid content of rhCol III

Amino acid (AA)	AA number per repeat unit	Theoretical absolute content/mg/mL	Actual absolute content/mg/mL
Gly	10	0.20	0.19
Glu	3	0.12	0.11
Arg	3	0.14	0.14
Ala	4	0.09	0.10
Pro	6	0.18	0.18
Phe	1	0.04	0.04
Asn	1	0.04	0.03
Ile	1	0.03	0.03
Lys	1	0.04	0.040
Total	30	0.87	0.86

Fig. 3 FTIR spectra of rhCol III and bCol I

Table 4 FTIR spectra characteristic peaks of bCol I and rhCol III

	Amide A/cm^{-1}	Amide B/cm^{-1}	Amide I/cm^{-1}	Amide II/cm^{-1}	Amide III/cm^{-1}	Amide III/A1450
bCol I	3,305	2,920	1,653	1,545	1237	1.08
rhCol III	3,291	2,963	1,653	1,542	1240, 1260	0.93, 1.00

cell adhesion, proliferation, migration, and functional expression [38, 39]. As previously described, abundant cellular recognition sites were contained in rhCol III [30], some of which could interact with multiple receptors on the cell surface. These interactions might affect a series of biological behaviors of the HSF [40, 41].

3.2.1 Cell adhesion

As one of the main interactions between cell and matrix, cell adhesion was generally firstly determined to clarify the specific interactions. In this study, bCol I was used as a positive control to investigate the influence of rhCol III on HSF adhesion. As the results shown in Fig. 4, only a few adhered cells were observed in the PBS group, in which BSA shielded the majority of non-specific sites on the plate and phosphate did not interact specifically with fibroblasts. In comparison, the cell adhesions in both rhCol III and bCol I groups were significantly higher than that in PBS group. Meanwhile, the cell adhesion in bCol I group was insignificantly lower than that in the rhCol III group ($p < 0.1086$). The different cell adhesion performance in two groups might be caused by the distinct proportion of "bioactive sites" such as integrin recognition sites in bCol I and rhCol III. The rhCol III with a specifically chosen amino acid sequence contained a higher proportion of integrin recognition sites compared with that in bCol I, while evidences indicated that bCol I preserved a higher content of the triple helix structure.

3.2.2 Cell proliferation

Both cytotoxic and the influence of rhCol III on HSF proliferation could be evaluated by CCK-8 assay, and the relative growth rates (RGR) of different groups were shown in Fig. 5. According to the cytotoxic evaluation criteria, the RGR in the rhCol III containing groups were all higher than that in the blank control group at all inspection time points, which meant rhCol III was nontoxic on HSF. Meanwhile, the cell proliferation increased in different concentrations of rhCol III containing groups with maximum RGR appearing in distinct culture courses. Specifically, the RGR increased in the whole culture course of 7 days in the low rhCol III concentration group (0.01 mg/ml), while the maximum RGR was achieved in 5 days and 3 days in middle concentration (0.1 mg/ml) and high concentration (1.0 mg/ml) groups, respectively. Therefore, it could be considered that rhCol III was positive in promoting cell proliferation, and the high rhCol III concentration could obviously accelerate cell proliferation in the short term. In contrast, the low rhCol III concentration could promote cell proliferation in a mild but long-lasting pattern, leading to the highest RGR among all groups.

3.2.3 Cell migration

Cell migration was a highly integrated and complex process that was a fundamental empirical investigation in biomedical application research. Wound healing in vivo was dominated by multiple factors, among which the migration rate of the cell was likely to play a crucial role
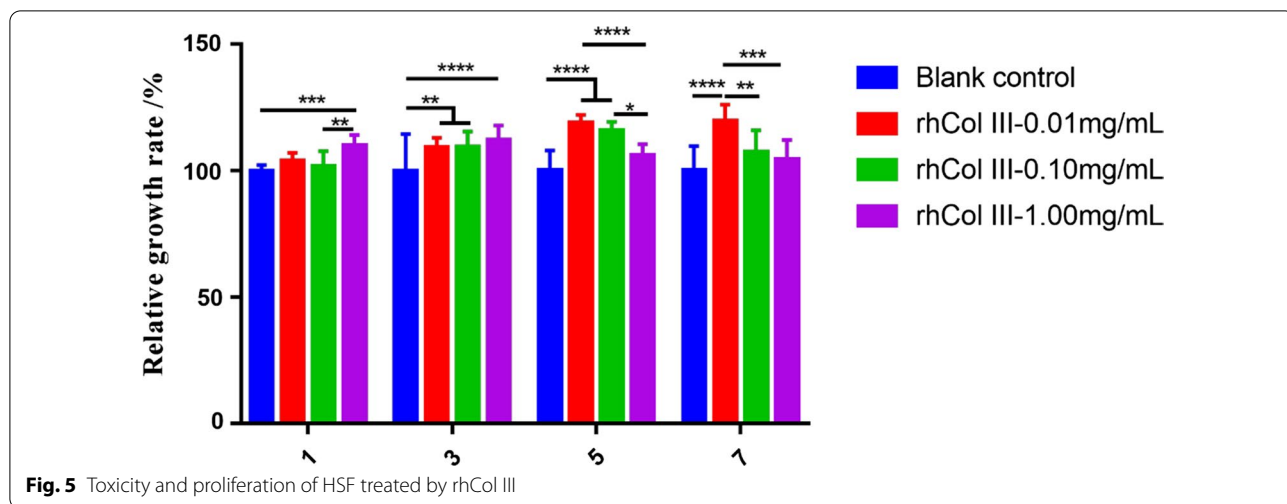

Fig. 4 HSF adhesion in different groups
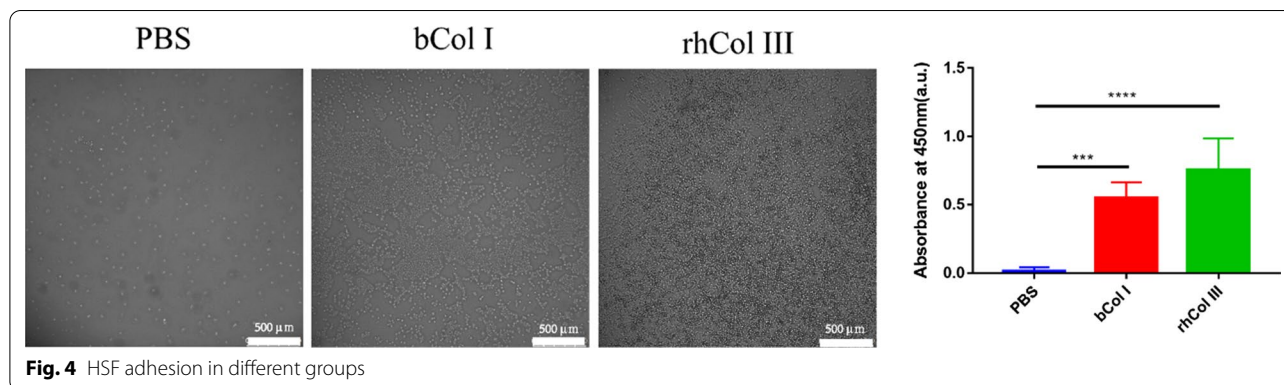
Fig. 5 Toxicity and proliferation of HSF treated by rhCol III

[42]. Cell migration was regulated by the local micro-environment, such as ECM rigidity, signaling factors and ligands on the ECM [43]. Although fast cell migration was not optimal for tissue repair, it could accelerate wound closure to reduce infections and the onset of pain and achieve a shortened healing period [44]. Cell scratch assay was applied to investigate the influence of rhCol III on HSF migration in vitro in this study. Figure 6a, b showed the pictures of HSF migration and the corresponding relative migration rates for the blank and rhCol III groups, respectively. The relative migration rate of rhCol III group was 38.63% after culturing for 24 h, which was significantly higher than that of the blank control group (16.02%). The confluence in rhCol III group was around 97.10% at 72 h, while that in the blank control

group was only 63.19%, suggesting an evidently positive influence of rhCol III on HSF migration ($p < 0.01$).

3.3 Influence of rhCol III on cell phenotype

It was reported that abundant integrin recognition sites and advanced structures similar to the native triple helix could endow recombinant collagen with a better biological activity to regulate the cell phenotype [45]. Collagen family and hyaluronic acid were the main components of skin ECM [46, 47], and the effective modulation of these ECM could potentially improve poor tissue defect repair.

3.3.1 Gene expression

To analyze the influence of rhCol III on HSF gene expression, TGF-β was chosen as a positive control because of

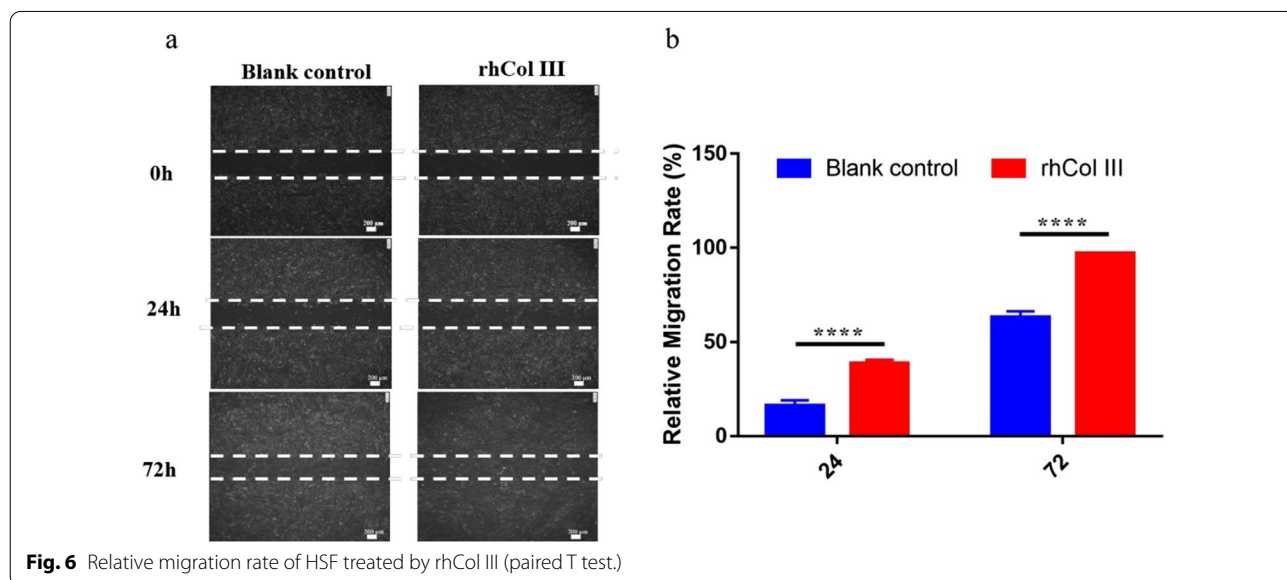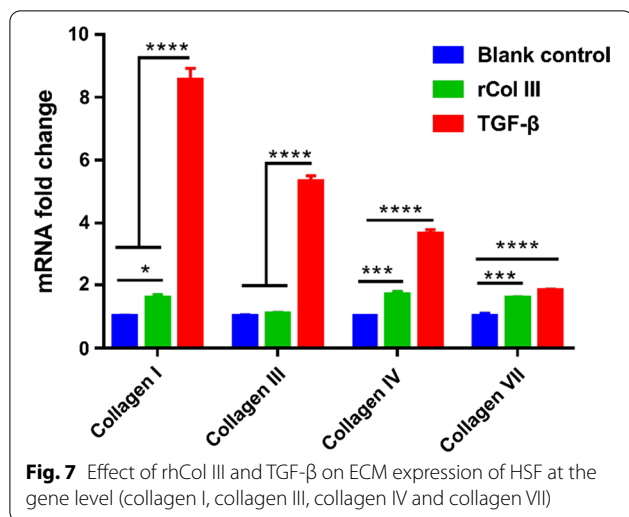**Fig. 6** Relative migration rate of HSF treated by rhCol III (paired T test.)

Wang *et al. Journal of Leather Science and Engineering*   (2022) 4:33

Page 9 of 13

Fig. 7 Effect of rhCol III and TGF-β on ECM expression of HSF at the gene level (collagen I, collagen III, collagen IV and collagen VII)

its well-known stimulation of fibroblasts. As the results of RT-qPCR shown in Fig. 7, the gene expression of collagen type I, type IV and type VII increased 59.00%, 70.33% and 59.33% in rhCol III group, respectively. Moreover, the increase was significant compared with the gene expression in the blank group at the same time point. At the same time, the collagen type III gene was insignificantly up-regulated in rhCol III group compared with the blank group. It was reported that collagen type III was firstly expressed preceding other collagen subtypes during the wound healing process [48]. The introduction of exogenous human gene encoded collagen type III segments might not increase the expression of Col III and construct a suitable cell microenvironment for further functional expression, which was beneficial for the expression of other ECM components and accelerated wound healing. As a widely used cell stimulator, TGF-β up-regulated all four subtypes of collagen obviously without selectivity, which might increase the risk of collagen over-expression. In contrast, rhCol III could mildly and selectively up-regulate the gene expression, which might be an important advantage in the application.
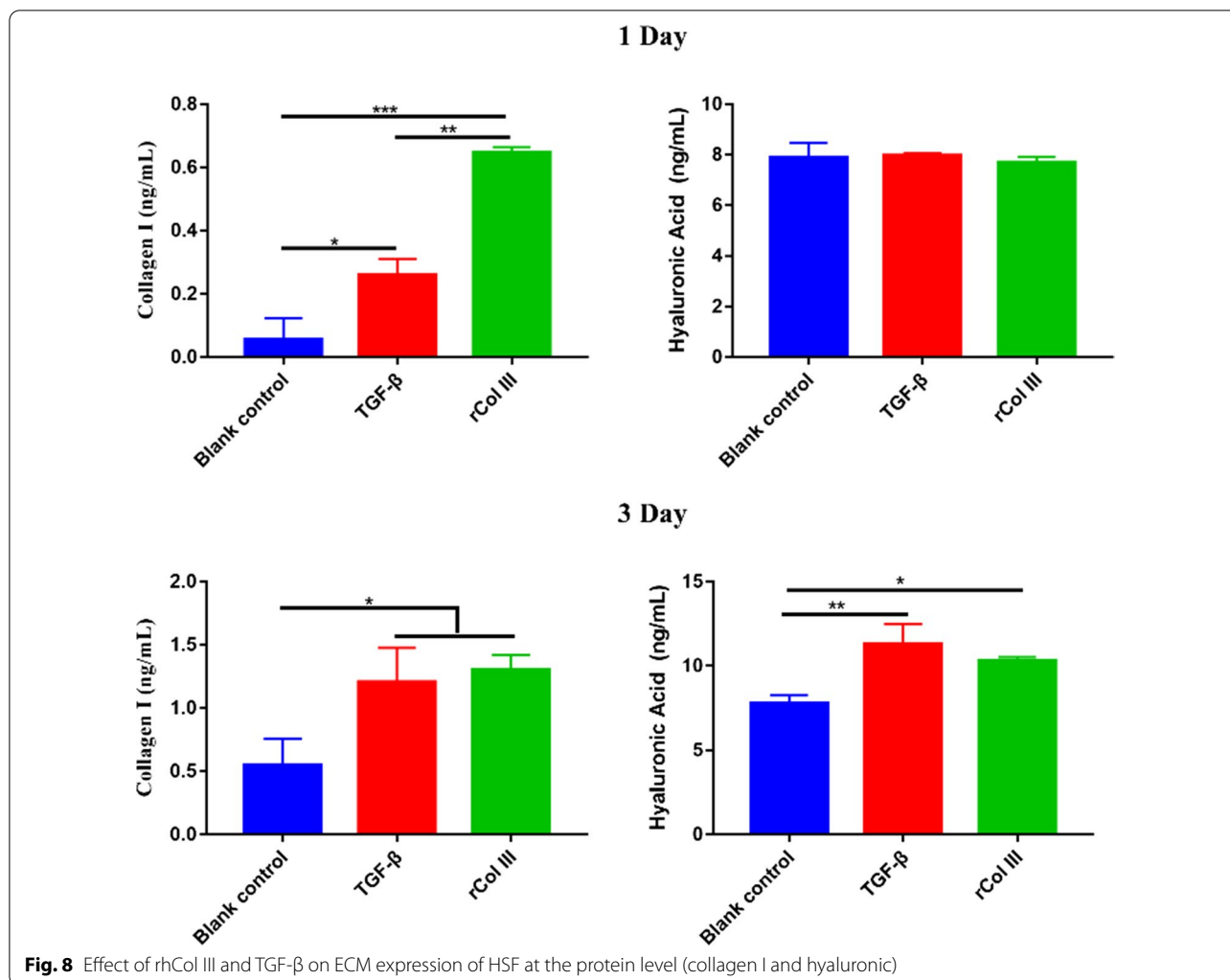
3.3.2 ECM expression

ELISA assay was used to analyze the effect of rhCol III on the expression of type I collagen and hyaluronic acid. On the first day, the results of ELISA (Fig. 8) showed that both rhCol III ($p < 0.001$) and TGF-β ($p < 0.05$) significantly enhanced the expression of type I collagen. Moreover, the expression of type I collagen in the rhCol III group was 2.65 times higher than that of TGF-β. However, the three experimental groups regarding hyaluronic acid content ranged from 7.701–7.902 ng/mL, and there was no significant difference among all three groups. Up to the third day, the content of type I collagen in the

three experimental groups was increased compared to the first day. The content of type I collagen in the rhCol III ($p < 0.05$) and TGF-β ($p < 0.05$) groups were still higher than that of the blank control group, but there was no significant difference between each of them. Intriguingly, there was a significant increase in hyaluronic acid expression in the rhCol III ($p < 0.05$) and TGF-β groups ($p < 0.01$). Although the TGF-β group had the highest amount of hyaluronic acid, the rhCol III and TGF-β groups had similar amounts of hyaluronic acid and showed no significant differences. The above two sets of data validated that rhCol III could promote the secretion of ECM at the gene and protein levels, which was compelling evidence for rhCol III as a prospective candidate to be used for tissue repair and regeneration.

4 Discussion

As a major component of the ECM, collagen not only contributes to the mechanical strength of tissues but also participates in the regulation of inflammation and promotes angiogenesis and ECM remodeling during tissue injury repair [49]. Collagen type III, an important member of the collagen superfamily, consists of three identical left-handed helix α1 chains twisted together to form a right-handed superhelix, the so-called triple helix [50]. During the early stage of wound repair, increased expression of collagen type III forms a temporary matrix that directs inflammatory cells and fibroblasts to the wound site [51].

It is known that native collagen has a hierarchical structure, which is crucial for molecular recognition and collagen function. The components and structural properties of rhCol III were verified by HPLC–MS, amino acid content analysis, FTIR and CD spectroscopy. The HPLC–MS results showed that the molecular weight of rhCol III was consistent with the theoretical design. The amino acid content analysis further demonstrated that rhCol III was correctly expressed and purified. The amino acid sequence served as the primary structure of rhCol III, and its correct expression was beneficial for the assembly of advanced structures and the correct recognition of multiple cellular receptors [52]. The CD spectroscopy results showed that rhCol III had characteristic negative and positive peaks, respectively, similar to that of the native collagen. FTIR further demonstrated that rhCol III had the feature of the triple helix and hydrogen bonds were engaged in the maintenance of the triple helix structure [37]. The rhCol III sequence was composed of a high proportion of amino acid sequences with staggered positive and negative charges, such as GEK, GER, which may cause the formation of axial charge pairs between the collagen chains. To some extent, this facilitated the stabilization of the triple helix structure even

Wang *et al. Journal of Leather Science and Engineering* (2022) 4:33

Page 10 of 13

Fig. 8 Effect of rhCol III and TGF-β on ECM expression of HSF at the protein level (collagen I and hyaluronic)

without proline hydroxylation [53]. Jeffrey D. Hartgerink etc. reported that protein chains could assemble into triple helix structures by a specific manner of electrostatic interactions [54], which might be caused by the side chain's charge magnitude and spatial structure. Although this specific interchain interaction might be a significant reason for forming the triple helix structure in rhCol III, the absence of hydroxyproline markedly reduced the triple helix content in rhCol III than that in animal-derived collagen, as showed by CD and FTIR spectra.

The preliminary results suggested rhCol III exhibited an excellent promotion effect on HSF adhesion, proliferation and migration. The cell-material interactions might be sophisticated and the possible reasons could be explained as following. As the major receptor family on the cell surface, integrins were responsible for cell adhesion to the surrounding extracellular matrix. rhCol III contained abundant integrin recognition sites, such as GAPGER, which accounted for about 60% of the entire

sequence [30]. The content of the integrin recognition sequence in rhCol III was significantly higher than that of bCol I, leading to a higher probability of interacting with integrins. This meant that rhCol III had a higher probability of interacting with integrins. It was reported in literatures that collagen and its derivatives could promote cell proliferation directly or indirectly because of the interaction between collagen and integrins α1β1 and α11β1 on the cell surface [55–57]. The migration of cells was achieved by a continuous cycle of multi-step cellular behavior, which included cell edge protrusion, ECM adhesion, cell body contraction, and cell tail de-adhesion [58]. Cell adhesion to the substrate material was critical for the cytoskeleton to generate the force that would drive cell migration [59]. However, cell adhesion activity and migration velocity were not a linear relationship, and the fastest migration velocity results from a net adhesion level of intermediate strength. As previously described

Wang *et al. Journal of Leather Science and Engineering*   (2022) 4:33

Page 11 of 13

for the cell migration step, the increased adhesion slowed the detachment of the cell tails from the substrate [60].

As one of the most abundant cells in connective tissues, the primary function of fibroblasts is to produce ECM for engaging in dynamic tissue remodeling [10]. Skin regeneration is limited by tissue modulation and repair capabilities, which may lead to defective ECM remodeling and massive loss of the original tissue structure and function [22]. Based on the current RT-qPCR and ELISA results, it could be hypothesized that the bioactive sites in rhCol III could be recognized by receptors on cell surface, had a positive interaction with HSF and further promoted the secretion of ECM at the gene and protein levels. The collagen I expression was not synchronously up-regulated as gene expression in TGF-β group on the first day and gradually increased on the third day according to the ELISA results, since the change of protein expression was generally delayed to that of gene expression. In rhCol III group, it could be hypothesized that rhCol III interacted with cells via surface receptor integrin, which could mainly influence cell adhesion and proliferation. Therefore, the up-regulation of collagen I gene in rhCol III group was not as obvious as that in TGF-β group, while the protein expression was greatly maintained on the first day leading to a higher collagen I expression. Because the strong influence of growth factor on cell phenotype, the ECM expressions were eventually increased to a comparable or even higher level than those in rhCol III group. These results demonstrated that rhCol III had excellent potential to promote fibroblast extracellular matrix expression, especially in the early stages. The literature reported that GAPGER, a segment in rhCol III, was the binding motif for integrin α2β1 [23], the binding of which could enhance collagen synthesis in fibroblasts [61]. Meanwhile, several studies had demonstrated that there was a similar upregulation trend of hyaluronic acid when collagen expression was up-regulated by stimulating fibroblasts [62].

5 Conclusion

The rhCol III characterized in this study conformed to the theoretical design from both component and structure aspects. As suggested by CD and FTIR spectra, the rhCol III chains could assemble into a triple helix structure which was similar to animal-derived collagen. The in vitro cell culture with rhCol III indicated that rhCol III had a noticeable influence on HSF behaviors as well as cell phenotype. Specifically, rhCol III significantly promoted cell adhesion, proliferation, and migration. At the same time, it enhanced the secretion of collagen and hyaluronic acid. The mechanism of cell-material interaction was not clearly understood yet, but it might be closely related to the similar triple-helix structure to native collagen and abundant integrin recognition sites in rhCol III. More molecular biology tests would provide more solid evidence in the future, which would support rhCol III as a prospective candidate for tissue repair and regeneration.

Author contributions
JW: Data curation, formal analysis, investigation, writing—original draft; HH: Methodology, visualization; JW: Data curation, formal analysis; HQ: investigation, visualization; YLG: formal analysis, investigation, writing—original draft; YX: investigation, software, visualization; ZHL: methodology, visualization; YJT: investigation, resources; LS: investigation, visualization; JR: Manuscript revision; HL: conceptualization, formal analysis, funding acquisition, investigation, project administration, supervision, writing; XDZ: project administration, supervision. All authors read and approved the final manuscript.

Availability of data and materials
The authors declare that all the data supporting the findings of this study are available within the article.

Declarations

Consent for publication
All authors have given approval to the final version of the manuscript.

Competing interests
The authors declare no competing financial interests in this work.

Author details
[1]National Engineering Research Center for Biomaterials, Sichuan University, Chengdu 610064, Sichuan, China. [2]College of Biomedical Engineering, Sichuan University, Chengdu 610064, Sichuan, China. [3]Shanxi Jinbo Pharmaceutical Co., Ltd., Taiyuan 030031, Shanxi, China. [4]West China School/Hospital of Stomatology, Sichuan University, Chengdu 610064, Sichuan, China. [5]Swinburne University of Technology, Melbourne, Australia.

References

1. McLaughlin S, McNeill B, Podrebarac J, Hosoyama K, Sedlakova V, Cron G, et al. Injectable human recombinant collagen matrices limit adverse remodeling and improve cardiac function after myocardial infarction. Nat Commun. 2019;10(1):4866.
2. Borghi N, Lowndes M, Maruthamuthu V, Gardel ML, Nelson WJ. Regulation of cell motile behavior by crosstalk between cadherin- and integrin-mediated adhesions. Proc Natl Acad Sci. 2010;107(30):13324–9.

3. Arseni L, Lombardi A, Orioli D. From structure to phenotype: impact of collagen alterations on human health. Int J Mol Sci. 2018;19(5):1407.

4. Pakshir P, Alizadehgiashi M, Wong B, Coelho NM, Chen X, Gong Z, et al. Dynamic fibroblast contractions attract remote macrophages in fibrillar collagen matrix. Nat Commun. 2019;10(1):1850.

5. Cai L, Heilshorn SC. Designing ECM-mimetic materials using protein engineering. Acta Biomater. 2014;10(4):1751–60.

6. Yang Y, Campbell Ritchie A, Everitt NM. Recombinant human collagen/chitosan-based soft hydrogels as biomaterials for soft tissue engineering. Mater Sci Eng C. 2021;121:111846.

7. Que RA, Chan SWP, Jabaiah AM, Lathrop RH, Da Silva NA, Wang S-W. Tuning cellular response by modular design of bioactive domains in collagen. Biomaterials. 2015;53:309–17.

8. Meganathan I, Sundarapandian A, Shanmugam G, Ayyadurai N. Three-dimensional tailor-made collagen-like proteins hydrogel for tissue engineering applications. Biomater Adv. 2022;139:212997.

9. Yang Y, Ritchie AC, Everitt NM. Using type III recombinant human collagen to construct a series of highly porous scaffolds for tissue regeneration. Colloids Surf B. 2021;208:112139.

10. Liang H, Russell SJ, Wood DJ, Tronci G. A hydroxamic acid–methacrylated collagen conjugate for the modulation of inflammation-related MMP upregulation. J Mater Chem B. 2018;6(22):3703–15.

11. Que RA, Arulmoli J, Da Silva NA, Flanagan LA, Wang S-W. Recombinant collagen scaffolds as substrates for human neural stem/progenitor cells. J Biomed Mater Res Part A. 2018;106(5):1363–72.

12. He Y, Wang J, Si Y, Wang X, Deng H, Sheng Z, et al. A novel gene recombinant collagen hemostatic sponge with excellent biocompatibility and hemostatic effect. Int J Biol Macromol. 2021;178:296–305.

13. Du C, Wang M, Liu J, Pan M, Cai Y, Yao J. Improvement of thermostability of recombinant collagen-like protein by incorporating a foldon sequence. Appl Microbiol Biotechnol. 2008;79(2):195–202.

14. Yu Z, An B, Ramshaw JAM, Brodsky B. Bacterial collagen-like proteins that form triple-helical structures. J Struct Biol. 2014;186(3):451–61.

15. Li H, You S, Yang X, Liu S, Hu L. Injectable recombinant human collagen-derived material with high cell adhesion activity limits adverse remodelling and improves pelvic floor function in pelvic floor dysfunction rats. Biomater Adv. 2022;134:112715.

16. Chen F, Strawn R, Xu Y. The predominant roles of the sequence periodicity in the self-assembly of collagen-mimetic mini-fibrils. Protein Sci. 2019;28(9):1640–51.

17. Peterson CM, Helterbrand MR, Hartgerink JD. Covalent capture of a collagen mimetic peptide with an integrin-binding motif. Biomacromol. 2022;23(6):2396–403.

18. Strawn R, Chen F, Jeet Haven P, Wong S, Park-Arias A, De Leeuw M, et al. To achieve self-assembled collagen mimetic fibrils using designed peptides. Biopolymers. 2018;109(7):e23226.

19. Xu Y, Kirchner M. Collagen mimetic peptides. Bioengineering. 2021;8(1):5.

20. Eming SA, Martin P, Tomic-Canic M. Wound repair and regeneration: mechanisms, signaling, and translation. Sci Transl Med. 2014;6(265):265sr6-sr6.

21. Hynes RO. The extracellular matrix: not just pretty fibrils. Science. 2009;326(5957):1216–9.

22. Bax DV, Davidenko N, Gullberg D, Hamaia SW, Farndale RW, Best SM, et al. Fundamental insight into the effect of carbodiimide crosslinking on cellular recognition of collagen-based scaffolds. Acta Biomater. 2017;49:218–34.

23. Malcor J-D, Mallein-Gerin F. Biomaterial functionalization with triple-helical peptides for tissue engineering. Acta Biomater. 2022;148:1–21.

24. Carafoli F, Mayer Marie C, Shiraishi K, Pecheva Mira A, Chan Lai Y, Nan R, et al. Structure of the discoidin domain receptor 1 extracellular region bound to an inhibitory fab fragment reveals features important for signaling. Structure. 2012;20(4):688–97.

25. Zhou L, Hinerman JM, Blaszczyk M, Miller JL, Conrady DG, Barrow AD, et al. Structural basis for collagen recognition by the immune receptor OSCAR. Proc Natl Acad Sci USA. 2016;127(5):529–37.

26. Brondijk THC, Bihan D, Farndale RW, Huizinga EG. Implications for collagen I chain registry from the structure of the collagen von Willebrand factor A3 domain complex. Proc Natl Acad Sci. 2012;109(14):5253–8.

27. Brondijk THC, de Ruiter T, Ballering J, Wienk H, Lebbink RJ, van Ingen H, et al. Crystal structure and collagen-binding site of immune inhibitory receptor LAIR-1: unexpected implications for collagen binding by platelet receptor GPVI. Blood. 2010;115(7):1364–73.

28. Feitsma LJ, Brondijk HC, Jarvis GE, Hagemans D, Bihan D, Jerah N, et al. Structural insights into collagen binding by platelet receptor glycoprotein VI. Blood J Am Soc Hematol. 2022;139(20):3087–98.

29. Yang C, Sesterhenn F, Bonet J, van Aalen EA, Scheller L, Abriata LA, et al. Bottom-up de novo design of functional proteins with complex structural features. Nat Chem Biol. 2021;17(4):492–500.

30. Wang J, Qiu H, Xu Y, Gao Y, Tan P, Zhao R, et al. The biological effect of recombinant humanized collagen on damaged skin induced by UV-photoaging: an in vivo study. Bioact Mater. 2022;11:154–65.

31. Long L, Hu C, Liu W, Wu C, Lu L, Yang L, et al. Microfibrillated cellulose-enhanced carboxymethyl chitosan/oxidized starch sponge for chronic diabetic wound repair. Biomater Adv. 2022;135:112669.

32. Pires V, Pêcher J, Da Nascimento S, Maurice P, Bonnefoy A, Dassonville A, et al. Type III collagen mimetic peptides designed with anti- or pro-aggregant activities on human platelets. Eur J Med Chem. 2007;42(5):694–701.

33. Cosgriff-Hernandez E, Hahn MS, Russell B, Wilems T, Munoz-Pinto D, Browning MB, et al. Bioactive hydrogels based on designer collagens. Acta Biomater. 2010;6(10):3969–77.

34. Hua C, Zhu Y, Xu W, Ye S, Zhang R, Lu L, et al. Characterization by high-resolution crystal structure analysis of a triple-helix region of human collagen type III with potent cell adhesion activity. Biochem Biophys Res Commun. 2019;508(4):1018–23.

35. Walker DR, Alizadehmojarad AA, Kolomeisky AB, Hartgerink JD. Charge-free, stabilizing amide—π interactions can be used to control collagen triple-helix self-assembly. Biomacromol. 2021;22(5):2137–47.

36. Stani C, Vaccari L, Mitri E, Birarda G. FTIR investigation of the secondary structure of type I collagen: new insight into the amide III band. Spectrochim Acta Part A Mol Biomol Spectrosc. 2020;229:118006.

37. de Melo Oliveira V, Araújo Neri RC, do Monte FTD, Roberto NA, Costa HMS, Assis CRD, et al. Crosslink-free collagen from Cichla ocellaris: STRUCTURAL characterization by FT-IR spectroscopy and densitometric evaluation. J Mol Struct. 2019;1176:751–8.

38. Langhe RP, Gudzenko T, Bachmann M, Becker SF, Gonnermann C, Winter C, et al. Cadherin-11 localizes to focal adhesions and promotes cell–substrate adhesion. Nat Commun. 2016;7(1):10909.

39. Chen Q, Zhang D, Zhang W, Zhang H, Zou J, Chen M, et al. Dual mechanism β-amino acid polymers promoting cell adhesion. Nat Commun. 2021;12(1):562.

40. Zeltz C, Gullberg D. The integrin–collagen connection—a glue for tissue repair? J Cell Sci. 2016;129(4):653–64.

41. Kim JK, Xu Y, Xu X, Keene DR, Gurusiddappa S, Liang X, et al. A novel binding site in collagen type III for integrins α1β1 and α2β1*. J Biol Chem. 2005;280(37):32512–20.

42. Qin S, Clark RAF, Rafailovich MH. Establishing correlations in the en-mass migration of dermal fibroblasts on oriented fibrillar scaffolds. Acta Biomater. 2015;25:230–9.

43. Yang R, Huang J, Zhang W, Xue W, Jiang Y, Li S, et al. Mechanoadaptive injectable hydrogel based on poly(γ-glutamic acid) and hyaluronic acid regulates fibroblast migration for wound healing. Carbohydr Polym. 2021;273:118607.

44. Amberg R, Elad A, Rothamel D, Fienitz T, Szakacs G, Heilmann S, et al. Design of a migration assay for human gingival fibroblasts on biodegradable magnesium surfaces. Acta Biomater. 2018;79:158–67.

45. Siljander PRM, Hamaia S, Peachey AR, Slatter DA, Smethurst PA, Ouwehand WH, et al. Integrin activation state determines selectivity for novel recognition sites in fibrillar collagens. J Biol Chem. 2004;279(46):47763–72.

46. Naylor EC, Watson REB, Sherratt MJ. Molecular aspects of skin ageing. Maturitas. 2011;69(3):249–56.

47. Lo DD, Zimmermann AS, Nauta A, Longaker MT, Lorenz HP. Scarless fetal skin wound healing update. Birth Defects Res C Embryo Today. 2012;96(3):237–47.

48. Govindaraju P, Todd L, Shetye S, Monslow J, Puré E. CD44-dependent inflammation, fibrogenesis, and collagenolysis regulates extracellular matrix remodeling and tensile strength during cutaneous wound healing. Matrix Biol. 2019;75–76:314–30.

49. Mathew-Steiner SS, Roy S, Sen CK. Collagen in wound healing. Bioengineering. 2021;8(5):63.
50. Kuivaniemi H, Tromp G. Type III collagen (COL3A1): gene and protein structure, tissue distribution, and associated diseases. Gene. 2019;707:151–71.
51. Makuszewska M, Bonda T, Cieślińska M, Bialuk I, Winnicka MM, Niemczyk K. Expression of collagen type III in healing tympanic membrane. Int J Pediatr Otorhinolaryngol. 2020;136:110196.
52. Cheng H, Rashid S, Yu Z, Yoshizumi A, Hwang E, Brodsky B. Location of glycine mutations within a bacterial collagen protein affects degree of disruption of triple-helix folding and conformation*. J Biol Chem. 2011;286(3):2041–6.
53. Sarkar B, O'Leary LER, Hartgerink JD. Self-assembly of fiber-forming collagen mimetic peptides controlled by triple-helical nucleation. J Am Chem Soc. 2014;136(41):14417–24.
54. Gauba V, Hartgerink JD. Surprisingly high stability of collagen ABC heterotrimer: evaluation of side chain charge pairs. J Am Chem Soc. 2007;129(48):15034–41.
55. Erusappan P, Alam J, Lu N, Zeltz C, Gullberg D. Integrin α11 cytoplasmic tail is required for FAK activation to initiate 3D cell invasion and ERK-mediated cell proliferation. Sci Rep. 2019;9(1):15283.
56. Edgar S, Hopley B, Genovese L, Sibilla S, Laight D, Shute J. Effects of collagen-derived bioactive peptides and natural antioxidant compounds on proliferation and matrix protein synthesis by cultured normal human dermal fibroblasts. Sci Rep. 2018;8(1):10474.
57. Leitinger B, Hohenester E. Mammalian collagen receptors. Matrix Biol. 2007;26(3):146–55.
58. Thievessen I, Thompson PM, Berlemont S, Plevock KM, Plotnikov SV, Zemljic-Harpf A, et al. Vinculin–actin interaction couples actin retrograde flow to focal adhesions, but is dispensable for focal adhesion growth. J Cell Biol. 2013;202(1):163–77.
59. Charras G, Sahai E. Physical influences of the extracellular environment on cell migration. Nat Rev Mol Cell Biol. 2014;15(12):813–24.
60. Schmidt S, Friedl P. Interstitial cell migration: integrin-dependent and alternative adhesion mechanisms. Cell Tissue Res. 2009;339(1):83–92.
61. Yu Y, Wu H, Zhang Q, Ogawa R, Fu S. Emerging insights into the immunological aspects of keloids. J Dermatol. 2021;48(12):1817–26.
62. Malekmohammadi M, Tehrani HA, Aghdami N. Effect of adipose derived stem cell-conditioned medium in the expression and synthesis of hyaluronic acid in human dermal fibroblasts. Clin Biochemy. 2011;44(13, Supplement):S6.

Publisher's Note